Available online at www.sciencedirect.com
SCIENCE DIRECT
Journal of Colloid and Interface Science 281 (2005) 39–48
JOURNAL OF Colloid and Interface Science
www.elsevier.com/locate/jcis

Modeling Pb sorption to microporous amorphous oxides as discrete particles and coatings

Ming Fan [a], Thipnakarin Boonfueng [a], Ying Xu [a], Lisa Axe [a,*], Trevor A. Tyson [b]

[a] *Department of Civil and Environmental Engineering, New Jersey Institute of Technology, Newark, NJ 07102, USA*
[b] *Department of Physics, New Jersey Institute of Technology, Newark, NJ 07102, USA*

Received 21 May 2004; accepted 9 August 2004

Available online 15 September 2004

Abstract

Hydrous amorphous Al (HAO), Fe (HFO), and Mn (HMO) oxides are ubiquitous in the subsurface as both discrete particles and coatings and exhibit a high affinity for heavy metal contaminants. To assess risks associated with heavy metals, such as Pb, to the surrounding environment and manage remedial activities requires accurate mechanistic models with well-defined transport parameters that represent sorption processes. Experiments were conducted to evaluate Pb sorption to microporous Al, Fe, and Mn oxides, as well as to montmorillonite and HAO-coated montmorillonite. Intraparticle diffusion, a natural attenuating process, was observed to be the rate-limiting mechanism in the sorption process, where best-fit surface diffusivities ranged from 10^{-18} to 10^{-15} $cm^2\,s^{-1}$. Specifically, diffusivities of Pb sorption to discrete aluminum oxide, aluminum oxide-coated montmorillonite, and montmorillonite indicated substrate surface characteristics influence metal mobility where diffusivity increased as affinity decreased. Furthermore, the diffusivity for aluminum oxide-coated montmorillonite was consistent with the concentrations of the individual minerals present and their associated particle size distributions. These results suggest that diffusivities for other coated systems can be predicted, and that oxide coatings and montmorillonite are effective sinks for heavy metal ions.
© 2004 Elsevier Inc. All rights reserved.

Keywords: Lead; Sorption; Intraparticle diffusion; Hydrous aluminum oxide; Hydrous iron oxide; Hydrous manganese oxide; Oxide coating; Montmorillonite

1. Introduction

Heavy metals such as lead (Pb) released into the subsurface pose a threat to human health and the surrounding environment. Concerns about the detrimental effects have resulted in extensive research efforts to better understand processes involved in the fate and transport of these contaminants in subsurface systems. Substantial studies have shown that trace metals are strongly associated with the particulate phases in aquatic environments [1–6]. These particulate phases are composed of a diverse mixture of clay minerals, metal oxides, and organic matter. Therefore, the sorption of metals in natural aquatic and/or soil environments is expected to be complicated given the varying composition of the interfaces.

Amorphous oxide minerals of aluminum, iron, and manganese occur as coatings on other mineral surfaces or as discrete particles, and are persistent in aquatic environments [5,7–10]. They have large surface areas, porous structures, and an abundance of binding sites; therefore, they have a significant impact on contaminant mobility [11,12]. In the sorption of heavy metals to hydrous oxides, numerous studies have demonstrated that this process is a two-step one [13–28]: rapid adsorption of metal ions to the external surface is followed by slow intraparticle diffusion along the micropore walls of the oxide. Benjamin and Leckie [13] observed that adsorption of Cd, Zn, Cu, and Pb on amorphous iron oxyhydroxide was initially fast followed by a much slower second step. Barrow et al. [14] studied adsorption kinetics of Ni, Zn, and Cd on goethite and concluded

* Corresponding author. Fax: +1-973-596-5790.
E-mail address: axe@adm.njit.edu (L. Axe).

0021-9797/$ – see front matter © 2004 Elsevier Inc. All rights reserved.
doi:10.1016/j.jcis.2004.08.050

that the observed two-step kinetics corresponded to a fast initial adsorption reaction followed by slow diffusion of the metal ions into the goethite. Fuller et al. [15] found that sorption of arsenate on hydrous ferric oxide proceeded in two steps with a fast uptake on the exterior of the aggregate and a slow uptake limited by the rate of intraparticle diffusion. Papelis et al. [17] investigated cadmium and selenite adsorption on aluminum hydroxides and found uptake is controlled by intraparticle diffusion. Recently, Axe and co-workers [18,19,22–24,27] conducted a series of sorption studies that included Sr, Cd, Zn, and Ni on amorphous Al (HAO), Fe (HFO), and Mn (HMO) oxides. In addition to adsorption edges and isotherms, they used constant boundary condition (CBC) semi-batch experiments, where the bulk adsorbate concentration was maintained approximately constant for all times. They found intraparticle diffusion was an important and rate-limiting process in sorption. Scheinost et al. [25] measured Cu and Pb sorption as a function of ferrihydrite morphology, temperature, metal competition, and fulvic acid concentration over a period of two months, in which surface diffusion was recognized as the limiting process. Manju et al. [26] conducted an investigation into the sorption of heavy metals, including Pb, Hg, and Cd, from wastewater by polyacrylamide-grafted iron (III) oxide. Intraparticle diffusion of metal ions through pores was shown to be the rate-limiting step. For porous surfaces such as Al, Fe, and Mn oxides, where the average pore size is greater than or equal to 1.9 nm [18,22], the distribution falls into the IUPAC classification of micro- and mesopores which is based on gas–solid systems. However, in the aqueous phase, pore surfaces are hydrated, resulting in potentially layers of water adsorbed to these pore walls [29]. Therefore, the mesopores may act as micropores. Based on previous studies, intraparticle diffusion of heavy metals in hydrous oxides is a critical step in sorption and plays an important role in fate and transport of metal contaminants in subsurface environments.

Many studies have also revealed that hydrous iron, manganese, and aluminum oxide coatings substantially affect sorption behavior [3–5,10,30–38]. For example, Levy and Tamura [30] observed that aluminum oxide-coated montmorillonite exhibited calcium–magnesium exchange properties different from those of pure montmorillonite. Lion et al. [3] found Fe/Mn hydrous oxides and organic coatings controlled Cd and Pb sorption in the South San Francisco Bay estuary. Knocke et al. [31] reported in a review that Mn oxide potentially deposits on filtration media in water treatment facilities increasing Mn removal. Edwards and Benjamin [32] found that iron oxide-coated sand had similar properties to discrete Fe oxide in removing metals over a wide pH range. Van Benschoten et al. [33] observed that iron oxide surface coatings reduce metal extraction efficiency from sandy soils. Lothenbach et al. [35] showed that at pH $>$ 6 aluminum oxide-coated montmorillonite was more efficient in immobilizing heavy metals than untreated montmorillonite, while in more acidic soils (pH $<$ 5), untreated montmorillonite was expected to be a dominant surface. Naidja et al. [36] found tyrosinase sorption on hydroxyaluminum-montmorillonite increased with increasing coating from 1 to 5 mmol Al/g clay.

In this research, systematic studies were conducted to assess Pb sorption to microporous Al, Fe, and Mn oxides. Studies included long-term ones to investigate intraparticle surface diffusivities. In addition, Pb sorption on montmorillonite and HAO-coated montmorillonite was evaluated. Montmorillonite is one of the most prevalent clays in soils and sediments and possesses a large specific surface area [39,40]. A number of studies have been conducted with montmorillonite coated Al or Fe oxyhydroxide [41–43] to simulate natural settings; however, long-term sorption processes have not been investigated to the same extent as in discrete oxide systems. Therefore, Pb sorption was investigated for HAO-coated montmorillonite and compared to that of discrete oxide systems.

2. Materials and methods

Sorption studies were conducted with freshly precipitated oxides at 25 °C. All chemicals used in oxide precipitation were reagent grade and only Millipore-Q Type I deionized water was employed. All systems were prepared in carbonate-free environment by purging with N_2. HAO was synthesized according to the method described by Gadde and Laitinen [44] and others [45–47], by drop-wise addition of stoichiometric amounts of NaOH to aluminum nitrate solution which was aged for 4 h prior to the sorption experiment. Using the method detailed by Gadde and Laitinen [44], HMO was prepared by slowly adding manganese nitrate to alkaline sodium permanganate solution. The HMO suspension was then centrifuged, rinsed, and redispersed in sodium nitrate solution at pH 7 where it was aged for 16 h. HFO was precipitated as described by Dzombak and Morel [48]; briefly, NaOH is slowly added to $Fe(NO_3)_3$ solution. The suspension is aged with constant mixing for 4 h at a pH of 7 to 7.5. Additional details for synthesizing HAO, HFO, and HMO are described elsewhere [18,22]. Montmorillonite used in the study has been treated (Swy-2, Clay Mineral Society), and included removal of carbonate, iron and manganese oxides, and organic matter in accordance with Kunze and Dixon [49] and O'Day et al. [50]. HAO-coated montmorillonite was prepared by drop-wise addition of an $Al(NO_3)_3$ solution to the montmorillonite suspension, which was followed by pH adjustment to 7.0 with 0.5 M NaOH. The suspension was mixed for 2 h, centrifuged, washed repeatedly with deionized water, and then freeze-dried. In an effort to assess the capacity of montmorillonite for the coating, a range of Al loadings (0.09, 0.18, 0.27, 0.54, 0.81, and 1.08 g Al/g clay) were applied. Acidic ammonium oxalate was used to extract noncrystalline aluminum oxide [51,52]; the extractant was filtered and analyzed with atomic absorption spectrometry (AA) for total Al. The loading of 0.18 g Al/g montmorillonite (or 0.35 g

HAO/g montmorillonite) was selected as it represents a maximum coating capacity on montmorillonite.

Characterization of the hydrous amorphous oxides, montmorillonite, and HAO-coated montmorillonite included particle size analyses (PSA) using a Beckman–Coulter LS 230 analyzer, surface area evaluation by N_2-BET (Brunauer–Emmett–Teller), and potentiometric titration to assess the pH point of zero charge (pH_{pzc}). Oxide mineralogy was characterized by a Philips X'Pert X-ray diffraction (XRD) with Ni-filtered Cu $K\alpha$ radiation. Morphology of the oxides was studied by a Philips Electroscan 2020 environmental scanning electron microscope (ESEM) and a LEO 1530 VP field emission scanning electron microscope (FE-SEM). In addition, energy dispersive X-ray analysis (EDX) was used for elemental mapping of the mineral surfaces.

Two types of sorption experiments were conducted: (i) conventional short-term ones, and (ii) long-term studies designed to evaluate diffusivities. Stock solutions were tagged with ^{210}Pb; its activity in the samples of suspensions and filtrates was measured with a Beckman LS6500 multipurpose scintillation counter. Turbulent hydraulic conditions (Reynolds number $> 10^4$ with respect to the reactor diameter) were maintained in all experiments to minimize the external mass-transfer resistance. Procedures for short-term studies involved adsorption edges and isotherms to evaluate the effect of pH, ionic strength, and concentration. A $NaNO_3$ electrolyte was used to maintain the ionic strength of solutions, which ranged from 1.0×10^{-3} to 1.0×10^{-1}. Short-term adsorption studies were conducted in 250-ml Nalgene containers with a contact time of 4 h. In these experiments, contact times from less than 1 to 72 h revealed no change in the amount sorbed, indicating equilibrium or pseudo-equilibrium between the lead adsorbed to external surface of the oxides and that in the bulk aqueous phase. The long-term or constant boundary condition (CBC) experiments were used to study the slow sorption process of intraparticle surface diffusion. In these studies, the Pb ion concentration in the bulk aqueous phase was maintained approximately constant by continuously monitoring and adding adsorbate as needed [18,19,22]. Therefore, the adsorbate concentration on the external surface of the particle was maintained constant. All aqueous concentrations of Pb were below saturation based on MINEQL+.

3. Results and discussion

3.1. Oxide characteristics

Earlier studies [19,22] revealed discrete oxide aggregates were generally spherical with irregular topography. The coating shows increased aggregation as compared to discrete aluminum oxide and montmorillonite (Fig. 1). An analysis for Al and Si reveals that Al appears to be more abundant on the HAO-coated montmorillonite than the montmorillonite surface; on the other hand, the coating has less Si than montmorillonite (Fig. 2). XRD also confirms the presence of the HAO coating; although the montmorillonite structure was observed, its intensity decreased as the degree of coating increased. Furthermore, discrete HAO and montmorillonite systems have smaller modes in the particle size distribution (PSD) than the coated system (Fig. 3). The pH_{PZC} of the HAO-coated montmorillonite is 5.0 ± 0.5 (Table 1), which is consistent with Zhuang and Yu [37]. Avena and De Pauli [53] observed a pH_{PZC} of 8.5 for the edge sites of montmorillonite, where most of the pH-dependent charge is located [54,55]. The difference between our results and others lies in that edge sites only account for approximately less than 4% of the overall montmorillonite surface area. Given the pH_{PZC} of 8.6 for HAO and

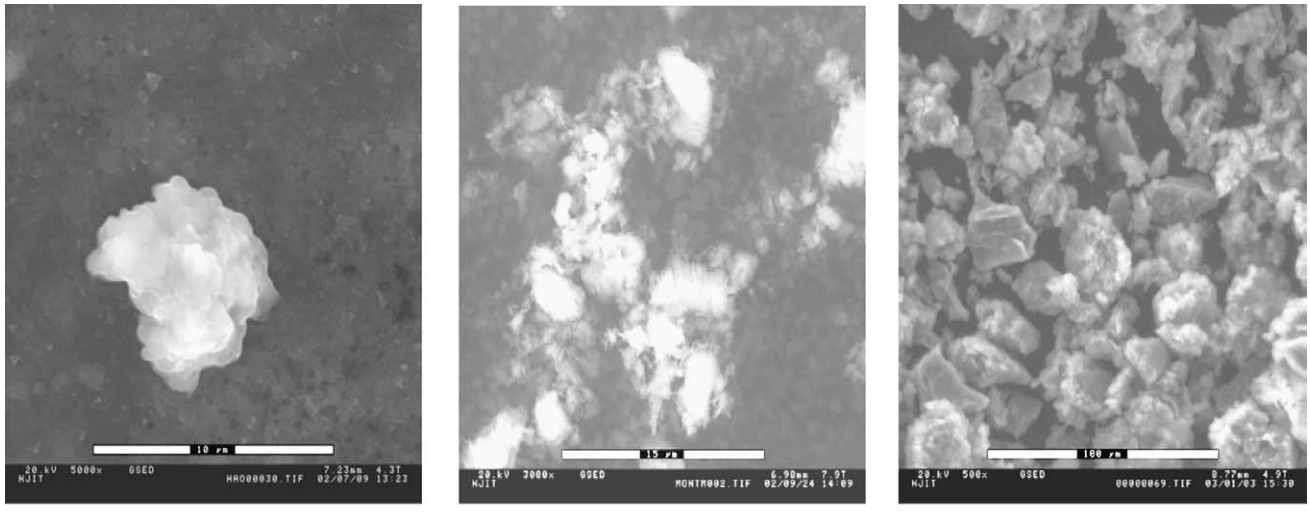

(a) HAO (b) montmorillonite (c) HAO-coated montmorillonite

Fig. 1. ESEM micrographs of HAO, montmorillonite, and HAO-coated montmorillonite.

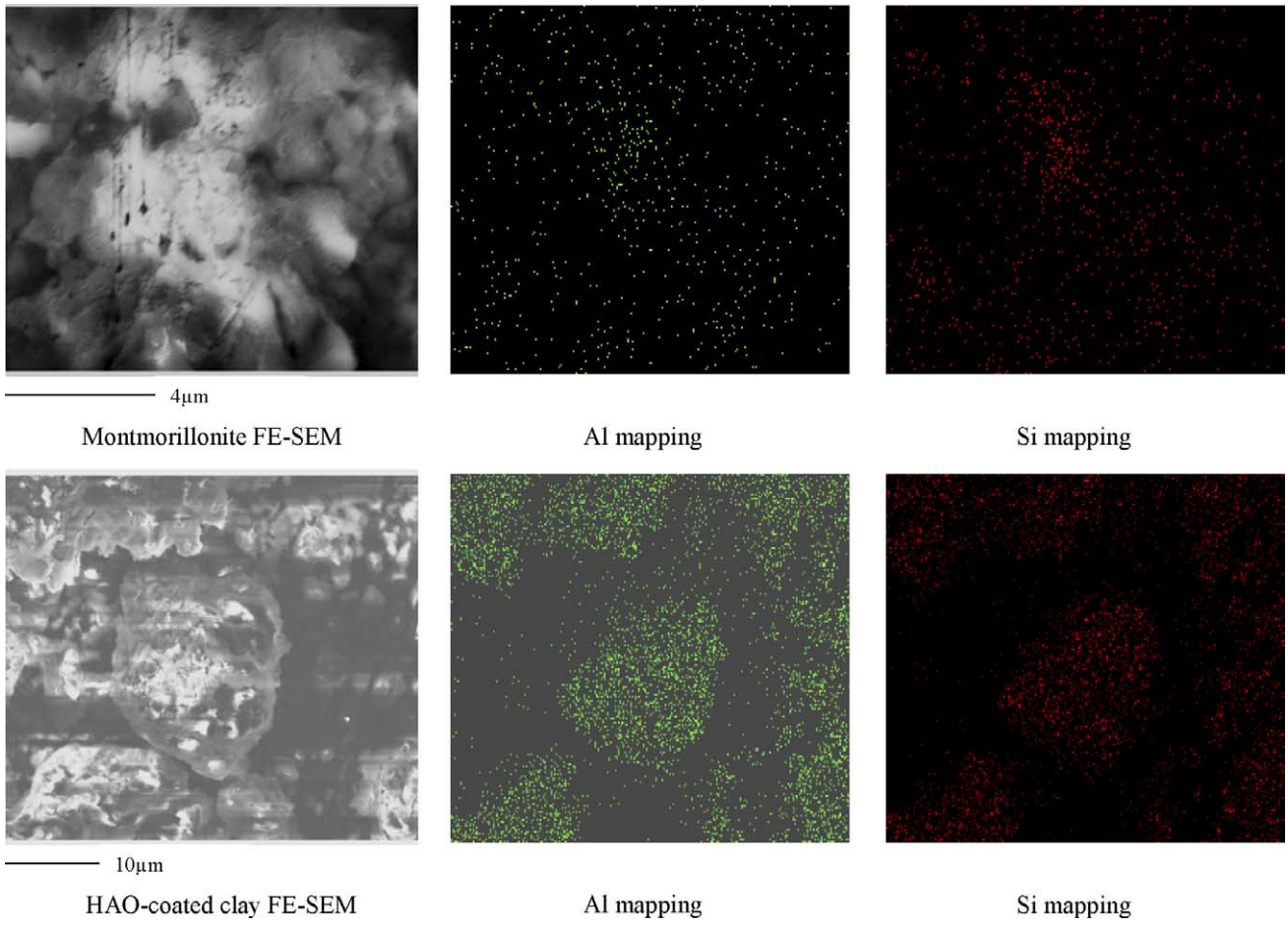

Fig. 2. EDX mapping of silicon and aluminum on HAO-coated montmorillonite and montmorillonite.

Table 1
Characteristics of HAO, HFO, HMO, montmorillonite, and HAO-coated montmorillonite

Materials	Surface area ($m^2\ g^{-1}$)	Porosity	Mode pore diameter (nm)	Mean diameter (μm)	Bulk density ($g\ cm^{-3}$)	pH_{PZC}	K (Pb adsorption) ($L\ mol^{-1}$)
HAO	411[a]	0.45	1.9	7.5	1.54	8.6 ± 0.5	1.4×10^3
HFO	600[b]	0.50	3.8	13.0	1.75	7.6 ± 0.5	4.0×10^4
HMO	359[a]	0.35	2.1 (Bimodal), 6.1	19.6	1.75	2.4 ± 0.5	3.9×10^6
Montmorillonite	27.8	0.51	8.7	8.7	1.48	4.2 ± 0.5	4.1×10^5
HAO-coated montmorillonite	10.1	0.72	17.8	21.8	1.03	5.0 ± 0.5	2.4×10^4

[a] Based on Trivedi and Axe [22].
[b] Based on Dzombak and Morel [48].

4.2 for montmorillonite determined experimentally, montmorillonite still plays a critical role in the surface charge of the coating system; this is most likely because of the nonuniform nature of the coating, which can be observed in the FE-SEM micrograph (Fig. 2). Other characteristics such as porosity, bulk density, and surface area are presented in Table 1. Montmorillonite has a large internal surface area that may not be accounted for in using N_2-BET; however, this does not significantly impact our modeling as sorption and the associated parameters were normalized to the mass present.

3.2. Sorption studies

In adsorption edge experiments with HFO (Fig. 4) there was no effect of ionic strength, suggesting Pb ions may form inner-sphere complexes with this surface, which is consistent with other studies [56,57]. Swallow et al. [57] reported

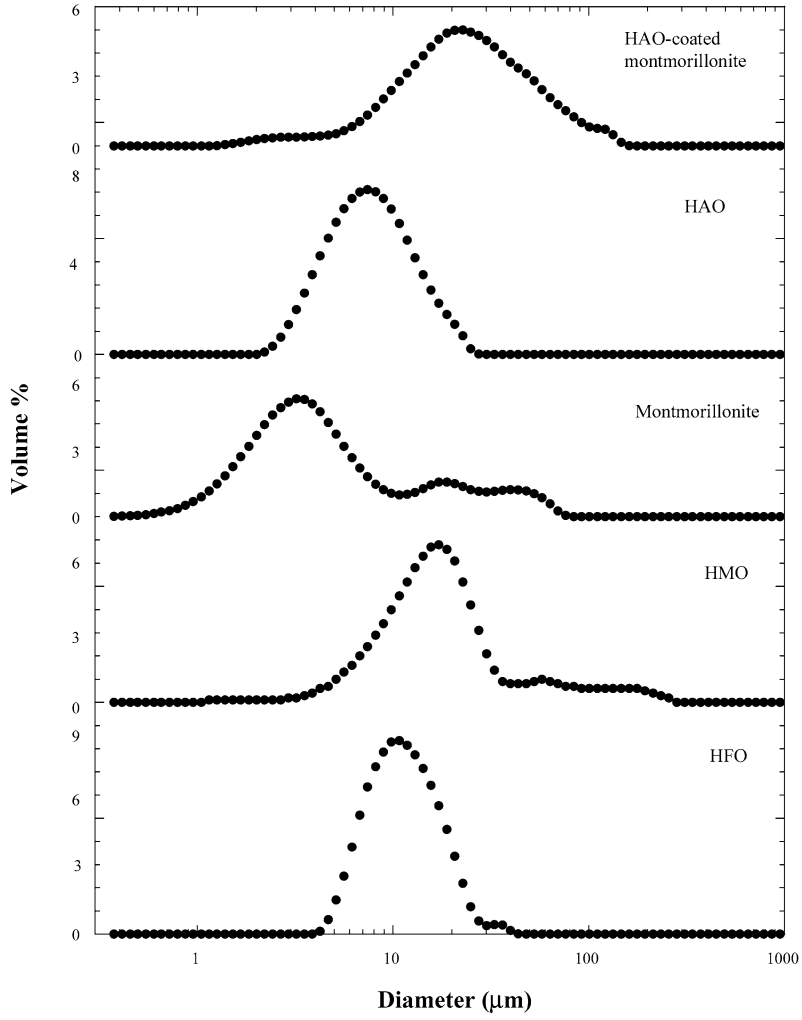

Fig. 3. Particle size distributions of HAO, HFO, HMO, montmorillonite, and HAO-coated montmorillonite at pH 5, ionic strength 1.0×10^{-2} M with $NaNO_3$, and 25 °C.

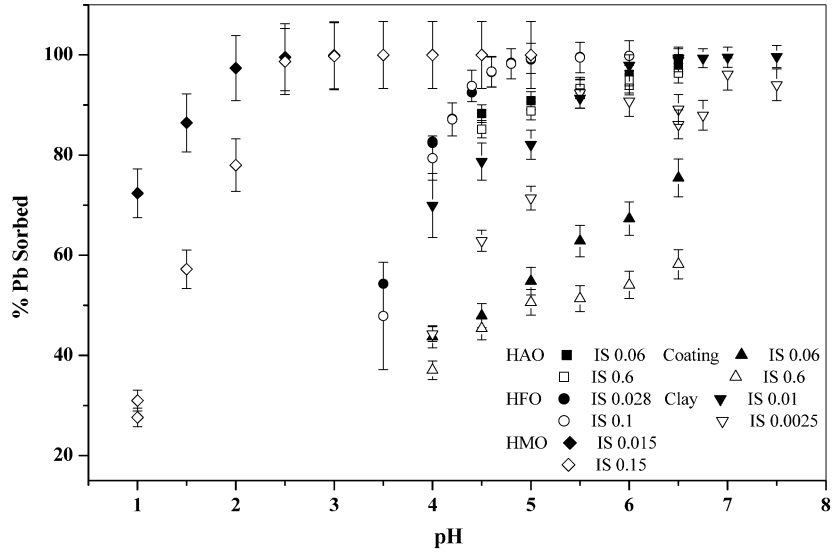

Fig. 4. Pb adsorption edges on HFO, HMO, HAO, montmorillonite, and HAO-coated montmorillonite, at 25 °C as a function of ionic strength with $NaNO_3$. For all Pb studies, the initial concentration was 10^{-5} M. HAO and HFO concentrations were 1 g L^{-1}, HMO concentration was 0.5 g L^{-1}, montmorillonite concentration was 0.001 g L^{-1}, and HAO-coated montmorillonite concentration was 0.005 g L^{-1}.

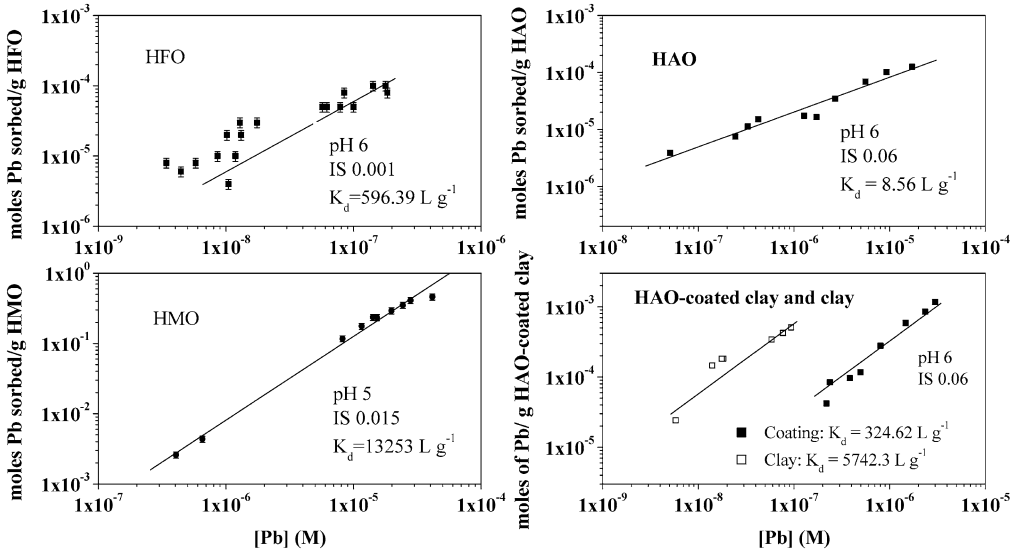

Fig. 5. Isotherms of Pb adsorption to HFO, HMO, HAO, montmorillonite, and HAO-coated montmorillonite at 25 °C with $NaNO_3$ electrolyte. HAO concentration was 0.5 g L^{-1}, HFO concentration was 0.3 g L^{-1}, HMO concentration was 0.5 g L^{-1}, montmorillonite concentration was 0.001 g L^{-1}, and HAO-coated montmorillonite concentration was 0.005 g L^{-1}.

that sorption of Cu^{2+} and Pb^{2+} to hydrous ferric oxide was unaffected by variations in ionic strength from 0.005 to 0.5 M $NaClO_4$, or by changes in the nature of the background electrolyte from $NaClO_4$ to a complex artificial seawater mixture. Trivedi et al. [56] observed that Pb sorption to ferrihydrite did not vary with ionic strength between 10^{-3} and 10^{-1} M $NaNO_3$. The adsorption edge for HAO begins at pH 4.5, a lower pH condition may result in dissolution; therefore, given the degree of adsorption, the effect of ionic strength may not be discernible. For Pb adsorption on HMO, montmorillonite, and HAO-coated montmorillonite, our results showed Pb sorption decreased with increasing ionic strength. Pb ions may form outer-sphere complexes on these surfaces. Other researchers [22,23,58,59] have found similar results. Among them, Trivedi and Axe [23] reported that Cd and Zn ions may retain their waters of hydration upon sorption to HAO, HFO, and HMO; compared with our investigations, amorphous oxides can form inner- or outer-sphere complexes with different metal ions. Other studies, for example, revealed Ni adsorption to Na-montmorillonite decreased with increase in ionic strength [58]. Furthermore, using XAFS (X-ray absorption fine structure spectroscopy), Strawn and Sparks [40] found Pb adsorption on montmorillonite varies from primarily outer-sphere complexation at low ionic strength and pH to a mixture of outer- and inner-sphere complexation as pH and ionic strength increase. Pb adsorption at high ionic strength (>0.1 M) may be associated with the permanently charged surface sites on the clay edges [40]. Because we observed an ionic strength effect suggesting outer-sphere complexation, Pb adsorption on montmorillonite at a relatively low ionic strength may involve ion exchange sites.

Isotherms for Pb adsorption to the three oxides, montmorillonite, and HAO-coated montmorillonite show a linear relationship between that sorbed to the external surface of the mineral and the bulk aqueous concentration (Fig. 5) suggesting adsorption can be described with one average type of site. Based on Langmuir–Hinshelwood kinetics and given that the available sites are approximately equivalent to the total sites, the Langmuir isotherm reduces to the linear distribution model [60]. The distribution coefficient K_d (L g^{-1}) is simply the product of the total sites and the equilibrium constant. This approach is useful for describing adsorption in modeling the long-term sorption process (discussed below). Among a number of macroscopic studies, Hiemstra et al. [61] used a single type of surface site to describe the titration behavior of hematite that exhibits poorly developed crystal planes. Christal and Kretzschmar [62] showed that the titration behavior as well as the adsorption of Cu and Pb to hematite could be described very well with a single surface site. Through XAFS, Manceau et al. [63] observed lead adsorbed to HFO by one mechanism, a mononuclear edge-sharing bidentate complex. Trivedi et al. [56] found the configuration of the sorption complex is independent of the adsorbate concentration at constant pH. Therefore, they concluded that Pb sorption to ferrihydrite may be described with one average type of mechanism. Based on our isotherms of Pb sorption on montmorillonite and HAO-coated montmorillonite, Pb sorption to the montmorillonite surface is greater than that for the coated one. On the other hand, Zhuang and Yu [37] also investigated similar systems but did not observe an effect of the Al oxide coating on sorption; this difference may be due to the degree of coating and that the isotherm was conducted at a different pH, 6.5. While edges and isotherms reveal effects of pH and concentration, they are short-term (4 h contact time) experiments resulting from adsorption to the external surface. For microporous sorbents, long-term studies are needed as well.

In these alternative experiments, a constant boundary condition was maintained, where the initial amount of Pb sorbed represents adsorption to the external surface. Pb concentrations employed in these experiments are within the linear range studied in the isotherm studies. Subsequently, the amount of Pb ion sorbed to the oxide gradually increased due to intraparticle surface diffusion. Initially, pore diffusion was considered in modeling sorption; however, predictions only accounted for 20% of the total sorbed when the bulk concentration at pore entrance is used as the boundary condition. Furthermore, the variance did not converge and therefore, pore diffusion cannot describe the experimental data. On the other hand, when adsorption is significant, transport in pores is dominated by surface diffusion [64]. For spherical particle geometry, a linear isotherm, and insignificant pore diffusion, the species mass balance for Pb is

$$\frac{\partial C}{\partial t} = \frac{D}{r^2}\frac{\partial\left[r^2\left(\frac{\partial C}{\partial r}\right)\right]}{\partial r}, \tag{1}$$

where

$$D = \frac{D_s}{1+\left(\frac{\varepsilon_p}{\rho K_i}\right)}. \tag{2}$$

In this expression, C is the contaminant concentration sorbed, D_s is the surface diffusivity and fitting parameter in the model, ε_p is the oxide porosity, ρ is the bulk density, and K_i is the distribution coefficient representing the equilibrium constant times the internal site density. The assumption that internal sites are no different than external ones has been observed in recent work with XAFS, for example, in Zn sorption to HMO the local structure from long-term samples was consistent with that from short-term samples [65]. In addition, XAFS work with Sr sorption to HMO [66] as well as HFO [67] further corroborates this assumption. Applying this assumption here for Pb sorption, the analytical solution to Eq. (1) integrated over the volume of a sphere based on the following initial and boundary conditions

$$C(r,0) = 0, \tag{3}$$

$$\frac{\partial C}{\partial r}(0,t) = 0, \tag{4}$$

$$C(R,t) = C_s \tag{5}$$

results in the mass sorbed per particle at a given time,

$$M = 4\pi C_s \frac{R^3}{3}\left[1 - \frac{6}{\pi^2}\sum_{n=1}^{\infty}\frac{1}{n^2}\exp\left(-\frac{Dn^2\pi^2 t}{R^2}\right)\right], \tag{6}$$

where C_s is the metal concentration sorbed on the oxide external surface. The amount sorbed to the internal surface of a single particle times the number of particles present for given radius (R) was summed over the entire particle size distribution to obtain the concentration sorbed internally. This total plus that sorbed to the external surface found from the short-term sorption studies provides the theoretical concentration. By minimizing the variance, the only fitting parameter is surface diffusivity; modeling results are shown in Figs. 6 and 7. Errors associated with the experiments were calculated from the propagation of errors (POE) method [68] and range from 7 to 10%. Errors associated with the model from POE method are also shown, which accounts for standard deviations in the number of particles as well as the error in the distribution coefficient describing the mass adsorbed to the surface. All data fall within two standard deviations of the model, which demonstrates the diffusion model fits data reasonably well. Furthermore, substantial evidence supports intraparticle diffusion as the rate-limiting mechanism in sorption to microporous oxides: Sr sorption to HFO [18] and HAO and HMO [22], Cu and Pb sorption to ferrihydrite [69], and Ni, Cd, and Zn sorption to HAO, HFO, and HMO [23,24]. Based on our adsorption isotherms and recent work with XAFS [65–67], there is no evidence of either surface precipitation or solid–solid solution formation; long-term studies suggested that internal surface sites were no different than external ones. In addition, given the presence of microporosity, intraparticle diffusion is expected and is therefore modeled as the rate-limiting process in Pb sorption to these oxides and coatings.

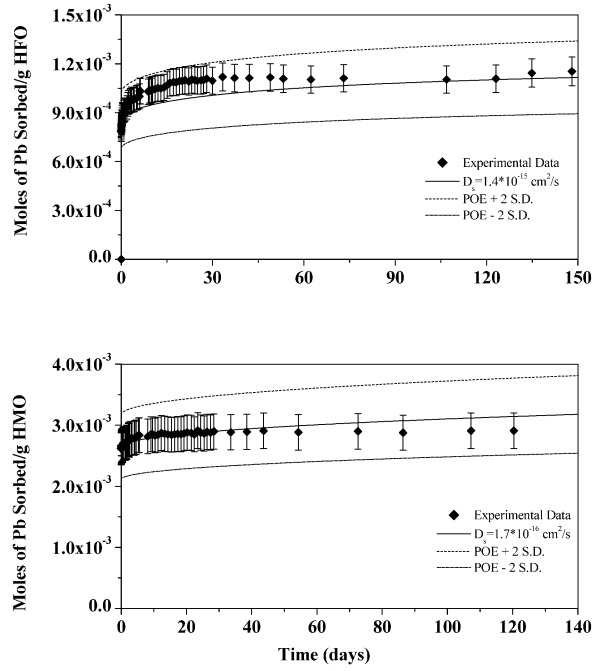

Fig. 6. CBC studies of Pb sorption to HFO and HMO at 25 °C with an ionic strength of 1.5×10^{-2} M ($NaNO_3$). For HFO, $[Pb]_{bulk} = 5.2 \times 10^{-5}$ M at pH 5 and 0.3 g L^{-1} HFO, and for HMO, $[Pb]_{bulk} = 4.4 \times 10^{-4}$ M at pH 4 and 0.1 g L^{-1} HMO.

Studies with Pb sorption to HFO, HMO, HAO, montmorillonite, and HAO-coated montmorillonite (Figs. 6 and 7) demonstrate that surface diffusivities range from 10^{-18} to 10^{-15} $cm^2\ s^{-1}$. These diffusivities clearly show that diffusion is a slow and rate-limiting process in sorption. After running the model to equilibrium, which takes approximately 15 to 30 years, internal sites were found to be responsible for approximately 45–90% of the total metal uptake to these oxides. For discrete oxides, surface diffusion is

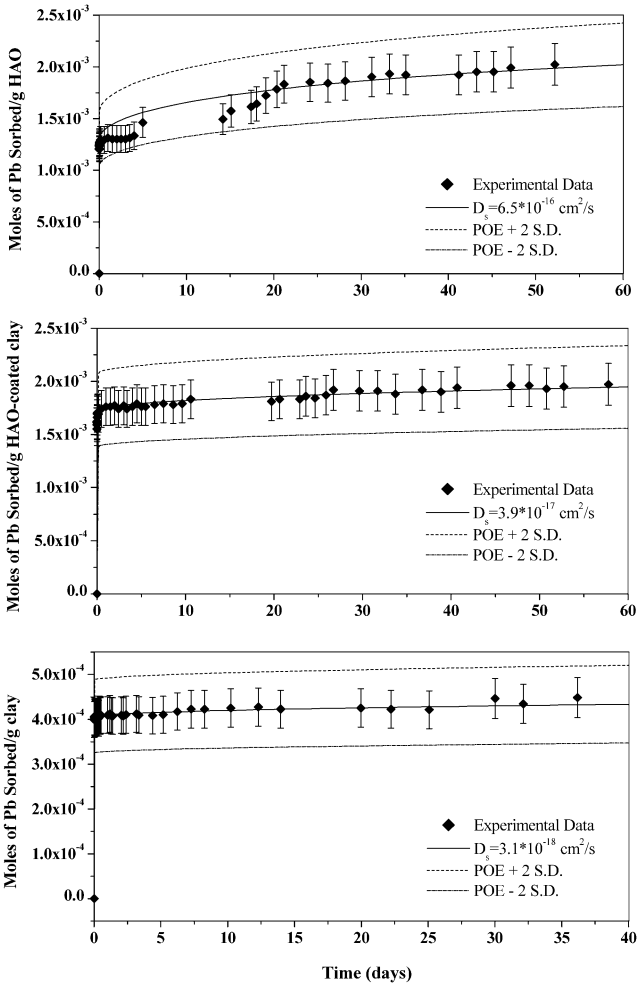

Fig. 7. CBC studies of Pb sorption to HAO, montmorillonite, and HAO-coated montmorillonite at 25 °C and an ionic strength of 1.0×10^{-2} M with $NaNO_3$. For HAO, $[Pb]_{bulk} = 8.3 \times 10^{-6}$ M at pH 6 and 0.02 g L^{-1} HAO; for HAO-coated montmorillonite, $[Pb]_{bulk} = 1.7 \times 10^{-4}$ M at pH 5 and 0.2 g L^{-1} coatings; and for montmorillonite, $[Pb]_{bulk} = 9.5 \times 10^{-6}$ M at pH 6 and 0.1 g L^{-1} montmorillonite.

the dominant mode of intraparticle transport, which is consistent with others [18,19,22–24,70]. For sorption to montmorillonite, Morrissey and Grismer [71] studied sorption of acetone, benzene, and toluene to pure clay minerals including kaolinite, illite, and Ca-montmorillonite; they found the process was limited by diffusion. Gemeay et al. [72] observed adsorption kinetics of metanil yellow dye, *p*-aminodiphenylamine (p-NH2-DPA), and benzidine by Na-montmorillonte, where again intraparticle diffusion was the rate-limiting mechanism. Furthermore, Fadali [73] reported the sorption of basic dyes (Basic Red) onto montmorillonite was intraparticle diffusion-controlled. For sorption to oxide coatings, intraparticle diffusion has also been observed in a number of studies [74–78]. Among them, Holmen and Gschwend [74] observed that slow diffusion controls the rate of sorption of hydrophobic organic compounds on quartzitic aquifer sands with iron oxyhydroxide and aluminosilicate (clay) coatings. Jain and Ram [75] investigated lead and zinc sorption on sediment which was mainly composed of sand and Fe/Mn oxides; they observed very slow diffusion of the adsorbed metals from the surface into the micropores. Merkle et al. [76] studied soluble Mn (II) removal by oxide-coated media including synthetically coated and naturally coated, in which surface diffusion was too the rate-limiting mechanism.

Based on the resultant diffusivities for discrete aluminum oxide, aluminum oxide-coated montmorillonite, and montmorillonite, specifically 10^{-16}, 10^{-17}, and 10^{-18} $cm^2\,s^{-1}$ (Fig. 7), respectively, substrate surface characteristics influence metal ion mobility. The smallest diffusivity reflects the surface characteristics of montmorillonite, which exhibited the greatest affinity for Pb ions among the three systems. When Pb ions sorbed on aluminum oxide-coated montmorillonite, surface diffusion is affected by both the discrete oxide and clay. Based on the FE-SEM micrograph (Fig. 2), diffusion occurs in both aluminum oxide and montmorillonite. Furthermore, based on this diffusivity, the contribution from discrete aluminum oxide and clay can be evaluated by employing their individual particle size distributions and concentrations. The results suggest 0.82 g amorphous oxide/g clay produce the overall diffusivity. Compared with that initially applied, 0.35 g HAO/g clay, the amorphous oxide appears to have a greater impact than that based on stoichiometry. Montmorillonite is comprised of Al (18% by weight), Si (23%), Fe (7%), and O (45%) based on XRF analyses. During the coating process, the system was initially at about pH 2 for 2 h and then adjusted to pH 7. We hypothesize that alumina in montmorillonite partially dissolves, then reforms as amorphous oxides, which can be demonstrated by the montmorillonite solubility. Al solubility in montmorillonite is controlled by gibbsite or amorphous aluminum hydroxide [79]. At pH 2–3, Ganor et al. [80] found gibbsite dissolved at a rate of 2.2×10^{-12} mol $m^{-2}\,s^{-1}$ based on column studies and therefore, this rate may include mass transfer limitations. However, we maintained a turbulent regime in the batch system, thus the dissolution rate may be greater than that observed in column studies. Furthermore, Lydersen et al. [81] found amorphous aluminum oxide dissolution can be described as a two-step process at pH 4.5: the dissolution was relatively fast during the first 2.7 h, and then a far slower rate followed for the remaining 24 h. Based on their model, $C(t) = C_0 e^{-0.45t}$, where $C(t)$ is concentration of $Al(OH)_{3(s)}$ present at time t, C_0 is initial concentration of $Al(OH)_{3(s)}$, approximately 50–60% of the amorphous aluminum oxide dissolves in the first 2 h. Given 0.15 g of montmorillonite were present in the studies, the coating system is projected to exhibit a 17–20% increase in the amorphous aluminum oxide from alumina dissolution, which is consistent with our estimation based on concentrations and particle size distributions. This result also demonstrates that oxides control Pb sorption in coated areas, while montmorillonite is the dominant surface at uncoated edge areas.

Because these long-term studies are time-consuming, theoretically based methods to predict diffusivities may be use-

Table 2
Theoretical parameters of Pb sorbed to hydrous metal oxides

Oxide	λ (nm)[a]	C_t (site density) (mol g^{-1})[b]	ΔH^0 (kcal mol^{-1})[c]	Exp. D_s (cm^2 s^{-1})	E_A (kcal mol^{-1})	α[d]
HAO	0.35	0.012	38.2	6.5×10^{-16}	16.8	0.4
HFO	0.24	0.025	41.4	1.4×10^{-15}	16.1	0.4
HMO	0.15	0.034	42.3	1.7×10^{-16}	17.1	0.4

[a] Calculated from oxide surface area and site density.
[b] Based on Trivedi and Axe [22].
[c] Based on correlation between ΔH^0_{ads} and R_H (hydrated radius) developed by Trivedi and Axe [24].
[d] α for transition metals is 0.80 for HAO, 0.68 for HFO, and 0.60 for HMO [24].

ful. Based on previous work [19,22–24], site activation theory can be applied for this purpose, where the sorbed ion or molecule vibrates at a site until it has sufficient energy, E_A (activation energy), to jump to the neighboring site. Accordingly, assuming a sinusoidal potential field along the pore surface, the surface diffusivity is a function of E_A and the mean distance between the sites (λ),

$$D_s = \lambda\left(\frac{E_A}{2m}\right)^{1/2}\exp\left(\frac{-E_A}{RT}\right), \tag{7}$$

where m is the molecular mass of the sorbing species and $\exp(-E_A/RT)$ is the Boltzmann factor. From the polanyi relation, E_A is linearly related to adsorption enthalpy, ΔH^0, through the proportionality constant α which was studied for transition and alkaline earth metals [23,24]. Using the experimental diffusivity, E_A was estimated by Eq. (7) and employing the polanyi relation, α for HAO, HFO, and HMO was obtained (Table 2). The results show that the polanyi constant for Pb adsorption to the three oxides is equivalent. This constant is expected to be equivalent for metals from the same group of the Period Table because of potentially similar sorption complexes formed with the oxides. Using the α obtained through this study, activation energies of other metals from Group 14 (IVA) may be calculated, and theoretical diffusivities can be predicted.

4. Summary

Lead sorption to hydrous amorphous Al (HAO), Fe (HFO), and Mn (HMO) oxides as well as to montmorillonite and HAO-coated montmorillonite can be described by a two-step process: rapid adsorption of metal ions to the external surface is followed by slow intraparticle diffusion along the micropore walls. Best-fit surface diffusivities ranged from 10^{-18} to 10^{-15} cm^2 s^{-1}. Specifically for Pb sorption on discrete aluminum oxide, aluminum oxide-coated montmorillonite, and montmorillonite, diffusivities of 10^{-16}, 10^{-17}, and 10^{-18} cm^2 s^{-1}, respectively, were observed. The results indicate substrate surface characteristics influence metal ion mobility, where diffusivity increased as affinity decreased. These studies demonstrate transient natural attenuating processes such as intraparticle diffusion need to be included in accurately describing the migration of heavy metals in subsurface environments.

Acknowledgments

This material is based upon work supported by the National Science Foundation under Grant BES 0089903. The authors also gratefully acknowledge support from the U.S. Army Sustainable Green Manufacturing program through the National Defense Center for Environmental Excellence (Contract DAAE30-98-C-1050) and the DuPont Young Professor Grant. The authors thank Wanchun Yuan for conducting preliminary experiments.

References

[1] K.K. Turekian, in: National Research Council (Ed.), Geochemistry of Atmospheric Radon and Radon Products, National Academy of Sciences Press, Washington, DC, 1977, p. 121.
[2] P.G. Brewer, in: J.P. Riley, G. Skirrow (Eds.), Chemical Oceanography, vol. 1, Academic Press, London, 1975, p. 415.
[3] L.W. Lion, R.S. Altmann, J.O. Leckie, Environ. Sci. Technol. 16 (1982) 660.
[4] R.E. Jackson, K.J. Inch, J. Contam. Hydrol. 4 (1989) 27.
[5] D. Dong, Y.M. Nelson, L.W. Lion, M.L. Shuler, W.C. Ghiorse, Water Res. 34 (2000) 427.
[6] L. Weng, E.J.M. Temminghoff, W.H. Van Riemsdijk, Environ. Sci. Technol. 35 (2001) 4436.
[7] E.A. Jenne, J.M. Zachara, in: K.L. Dickson, A.W. Maki, W. Brungs (Eds.), Fate and Effects of Sediment-bound Chemicals in Aquatic Systems, Pergamon Press, New York, 1984, Chap. 8.
[8] M. McPhail, A.L. Page, F.T. Bingham, Soil Sci. Soc. Am. J. 36 (1972) 510.
[9] W. Stumm, J.J. Morgan, Aquatic Chemistry, Chemical Equilibria and Rates in Natural Waters, Wiley, New York, 1996.
[10] D. Dong, X. Hua, Y. Li, J. Zhang, D. Yan, Environ. Sci. Technol. 37 (2003) 4106.
[11] E.A. Jenne, in: R.F. Gould (Ed.), Trace Organics in Water, American Chemical Society, Washington, DC, 1968, p. 337.
[12] B.R. Coughlin, A.T. Stone, Environ. Sci. Technol. 29 (1995) 2445.
[13] M.M. Benjamin, J.O. Leckie, J. Colloid Interface Sci. 79 (1981) 209.
[14] N.J. Barrow, J. Gerth, G.W. Brummer, J. Soil Sci. 40 (1989) 437.
[15] C.C. Fuller, J.A. Davis, G.A. Waychunas, Geochim. Cosmochim. Acta 57 (1993) 2271.
[16] G.A. Waychunas, B.A. Rea, C.C. Fuller, J.A. Davis, Geochim. Cosmochim. Acta 57 (1993) 2251.

[17] C. Papelis, P.V. Roberts, J.O. Leckie, Environ. Sci. Technol. 29 (1995) 1099.
[18] L. Axe, P.R. Anderson, J. Colloid Interface Sci. 175 (1995) 157.
[19] L. Axe, P.R. Anderson, J. Colloid Interface Sci. 185 (1997) 436.
[20] D.G. Strawn, A.M. Schidegger, D.L. Sparks, Environ. Sci. Technol. 32 (1998) 2596.
[21] D.R. Roberts, A.M. Scheidegger, D.L. Sparks, Environ. Sci. Technol. 33 (1999) 3749.
[22] P. Trivedi, L. Axe, J. Colloid Interface Sci. 218 (1999) 554.
[23] P. Trivedi, L. Axe, Environ. Sci. Technol. 34 (2000) 2215.
[24] P. Trivedi, L. Axe, Environ. Sci. Technol. 35 (2001) 1779.
[25] A.C. Scheinost, S. Abend, K.I. Pandya, D.L. Sparks, Environ. Sci. Technol. 35 (2001) 1090.
[26] G.N. Manju, K.A. Krishnan, V.P. Vinod, T.S. Anirudhan, J. Hazard. Mater. B 21 (2002) 221.
[27] L. Axe, P. Trivedi, J. Colloid Interface Sci. 247 (2002) 259.
[28] T.K. Sen, S.P. Mahajan, K.C. Khilar, Colloids Surf. A Physicochem. Eng. Aspects 211 (2002) 91.
[29] J. Karger, D.M. Ruthven, Diffusion in Zeolites, Wiley, New York, 1992.
[30] R. Levy, T. Tamura, Israel J. Chem. 11 (1973) 285.
[31] W.R. Knocke, J.R. Hamon, C.P. Thompson, J. AWWA (December 1988) 65.
[32] M. Edwards, M.M. Benjamin, J. Water Pollut. Control Fed. 61 (1989) 1523.
[33] J.E. Van Benschoten, R.E. Reed, M.R. Matsumoto, P.J. McGarvey, Water Environ. Res. 66 (1994) 1994.
[34] E.H. Rybicka, W. Calmano, A. Breeger, Appl. Clay Sci. 9 (1995) 369.
[35] B. Lothenbach, G. Furrer, B. Schulin, Environ. Sci. Technol. 31 (1997) 1452.
[36] A. Naidja, P.M. Huang, J.M. Bollag, J. Mol. Catal. A Chem. 115 (1997) 305.
[37] J. Zhuang, G. Yu, Chemosphere 49 (2002) 619.
[38] M.P. Papini, A. Bianchi, M. Majone, M. Beccari, Ind. Eng. Chem. Res. 41 (2002) 1946.
[39] M.L. Schlegel, A. Manceau, D. Chateigner, L. Charlet, J. Colloid Interface Sci. 215 (1999) 140.
[40] D.G. Strawn, D.L. Sparks, J. Colloid Sci. 216 (1999) 257.
[41] A.K. Helmy, E.A. Ferreiro, S.G. De Bussetti, Clays Clay Miner. 43 (1994) 444.
[42] R. Celis, L. Cox, M.C. Hermosin, J.J. Cornejo, Environ. Qual. 26 (1997) 472.
[43] H. Green-Pederson, N. Pind, Colloids Surf. A Physicochem. Eng. Aspects 168 (2000) 133.
[44] R.R. Gadde, H.A. Laitinen, Anal. Chem. 46 (1974) 2022.
[45] P.R. Anderson, M.M. Benjamin, Environ. Sci. Technol. 24 (1990) 692.
[46] M. McPhail, A.L. Page, F.T. Bingham, Soil Sci. Soc. Am. J. 36 (1972) 510.
[47] L.M. Shuman, Soil Sci. Soc. Am. J. 41 (1977) 703.
[48] D.A. Dzombak, F.M.M. Morel, J. Colloid Interface Sci. 112 (1986) 588.
[49] G.W. Kunze, J.B. Dixon, in: A. Kulte (Ed.), Pretreatment for Mineralogical Analysis, American Society of Agronomy/Soil Science Society of America, Madison, WI, p. 91.
[50] P.A. O'Day, G.E. Brown, G.A. Parks, J. Colloid Interface Sci. 165 (1994) 269.
[51] H.P. Blume, U. Schwertmann, Soil Sci. Soc. Am. Proc. 33 (1969) 438.
[52] D.A. Dzombak, F.M.M. Morel, Surface Complexation Modeling Hydrous Ferric Oxide, Wiley, New York, 1990.
[53] M.J. Avena, C.P. De Pauli, J. Colloid Interface Sci. 202 (1998) 195.
[54] F.-R.C. Chang, G. Sposito, J. Colloid Interface Sci. 178 (1996) 555.
[55] G. Sposito, The Chemistry of Soils, Oxford Univ. Press, New York, 1989.
[56] P. Trivedi, J.A. Dyer, D.L. Sparks, Environ. Sci. Technol. 37 (2003) 908.
[57] C.K. Swallow, D.N. Hume, F.M.M. Morel, Environ. Sci. Technol. 14 (1980) 1326.
[58] B. Baeyens, M.H. Bradbury, J. Contam. Hydrol. 27 (1997) 199.
[59] A.M.L. Kraepiel, K. Keller, F.M.M. Morel, J. Colloid Interface Sci. 210 (1999) 43.
[60] H.S. Fogler, Elements of Chemical Reaction Engineering, Prentice–Hall, NJ, 1992.
[61] T. Hiemstra, J.C.M. De Wit, W.H. Van Riemsdijk, J. Colloid Interface Sci. 133 (1989) 105.
[62] I. Christl, R. Kretzschmar, Geochim. Cosmochim. Acta 63 (1999) 2929.
[63] A. Manceau, L. Charlet, M.C. Boisset, B. Didier, L. Spadini, Appl. Clay Sci. 7 (1992) 201.
[64] G.F. Froment, K.B. Bischoff, Chemical Reactor Analysis and Design, Wiley, New York, 1990.
[65] P. Trivedi, L. Axe, T.A. Tyson, Environ. Sci. Technol. 35 (2001) 4515.
[66] L. Axe, T.A. Tyson, P. Trivedi, T. Morrison, J. Colloid Interface Sci. 224 (2000) 408.
[67] L. Axe, G. Bunker, P.R. Anderson, T.A. Tyson, J. Colloid Interface Sci. 199 (1998) 44.
[68] H.H.J. Ku, Res. Natl. Bur. Stand. C Eng. Instrum. 70 (1966) 263.
[69] A.C. Scheinost, S. Abend, K.I. Pandya, D.L. Sparks, Environ. Sci. Technol. 35 (2001) 1090.
[70] N.Z. Misak, H.F. Ghoneimy, T.N. Morcos, J. Colloid Interface Sci. 184 (1996) 31.
[71] F.A. Morrissey, M.E. Grismer, J. Contam. Hydrol. 36 (1999) 291.
[72] A.H. Gemeay, A.S. El-Sherbiny, A.B. Zaki, J. Colloid Interface Sci. 245 (2002) 116.
[73] Q.A. Fadali, Appl. Sci. Technol. 21 (2003) 935.
[74] B.A. Holmen, P.M. Gschwend, Environ. Sci. Technol. 31 (1997) 105.
[75] C.K. Jain, D. Ram, Water Res. 31 (1997) 154.
[76] P.B. Merkle, W.R. Knocke, D.L. Gallagher, J.C. Little, J. Environ. Eng. 123 (1997) 650.
[77] C.H. Lai, S.L. Lo, H.L. Chiang, Chemosphere 41 (2000) 1249.
[78] R.Y.J. Stefanova, J. Environ. Sci. Health Part A 36 (2001) 1287.
[79] H.M. May, D.G. Kinniburgh, P.A. Helmke, M.L. Jackson, Geochim. Cosmochim. Acta 50 (1986) 1667.
[80] J. Ganor, J.L. Mogollon, A.C. Lasaga, Geochim. Cosmochim. Acta 63 (1999) 1635.
[81] E. Lydersen, B. Salbu, A.B.S. Poleo, I.P. Muniz, Water Resour. Res. 27 (1991) 351.